Engineered Science
DOI: https://dx.doi.org/10.30919/es8d817

Investigating the Effect of the Curing-Induced Residual Stress on the Mechanical Behavior of Carbon Nanotube/Epoxy Nanocomposites by Molecular Dynamics Simulation

S. M. Rahimian-Koloor and M. M. Shokrieh*

Abstract

The representative volume elements and molecular dynamics (MD) simulation are frequently used to compute the mechanical behavior of polymer nanocomposites. In previous studies, the polymer curing process was often not considered in the simulation process, thus the effect of residual stresses imposed on nanoparticles, matrix, and the interphase material between the nanoparticles and the matrix were not studied. In the present paper, the effect of curing-induced residual stresses of the nanoparticle, matrix, and interphase material on the mechanical behavior of nanocomposites was studied in detail. A model of nanocomposites was constructed using an in-situ curing process by the MD simulation. The modulus of the nanocomposite is obtained as 3.75 GPa, indicating a 60% improvement compared to that of the pure polymer. The results of the tensile loading of nanocomposites show that the residual stress on CNT was obtained as -197 MPa which is 33% of the maximum value of the applied stress on nanocomposites. The MD model is validated by analysis of the mechanical behavior of the isolated CNT and pure polymer block under tensile loads as well as the CNT pullout simulation.

Keywords: Nanocomposites; CNT; Molecular Dynamics Simulation; Mechanical Response; Residual stress.
Received: 22 January 2022; Revised: 22 December 2022; Accepted: 05 February 2023.
Article type: Research article.

1. Introduction

In the past few decades, the superb properties of carbon nanotubes (CNTs) made them one of the novel nanostructures for the reinforcement of polymeric materials.[1] The CNT-reinforced polymers in the form of nanocomposite materials have found many applications in advanced industries such as microelectronics, aerospace, *etc*.[2] The excellent mechanical properties of the CNT in polymer-based nanocomposites would cause great improvement in the properties of the nanocomposites to suit them for applications that desire higher mechanical properties to sustain the load and boundary conditions.[3] Many studies have been performed to characterize the mechanical behavior of nanocomposites using the representative volume element (RVE) in a molecular dynamic (MD) simulation or finite element method (FEM).[4-7] Chen *et al.* used a modified embedded FE technique to model CNT/polymer nanocomposites to overcome the challenges in modeling nanocomposites with complex morphology.[8] Xiaoxin *et al.* studied the AC conductivity and dielectric properties of nanocomposites reinforced by CNT using numerical and experimental approaches.[9] Hassanzadeh-aghdam *et al.* used a micromechanical approach to study the thermo-mechanical behavior of hybrid titanium nanocomposites considering the effects of adding CNTs.[10] Li and Seidel used MD simulation and a multiscale modeling approach to study the CNT interface ability in load-transfer and mechanical behavior of CNT/cross-linked-polymer nanocomposites.[11] They showed that enhancement in microscale mechanical properties of nanocomposite directly depends on the load-transfer of the CNT-polymer interface, which improves by covalent functionalization at the interface. The interaction between nanofillers and polymer through a crosslinking process, which results in excessive residual stress is one of the important concerns that have not been fully covered in previous studies.[12,13] On the other hand, in a

Composite Research Laboratory, Center of Excellence in Experimental Solid Mechanics and Dynamics, School of Mechanical Engineering, Iran University of Science and Technology, Tehran, 16846-13114, Iran.
**E-mail:* Shokrieh@iust.ac.ir (M. M. Shokrieh)

nanocomposites RVE system, the presence of CNT with outstanding stiffness and strength properties makes CNT a quasi-rigid material embedded in the soft polymeric matrix. Such a physical combination and its effect on the crosslinking or curing process of the polymer during the fabrication of the nanocomposites should be considered in the analysis of the mechanical behavior of RVEs that are used for the mechanical characterization of nanocomposite materials.

The present study focused on the behavior of single-wall carbon nanotube and polymer in the form of a CNT/epoxy RVE system. The RVEs are constructed through an in-situ cross-linking process of epoxy in the presence of the embedded CNT using LAMMPS software and an in-house developed code. The mechanical behavior of the isolated CNT, pure epoxy, and the whole RVE along with the pull-out test of the embedded CNT are obtained and used for stress analysis of the RVE system.

2. Materials and Methods

The thermoset polymer matrix was composed of a stoichiometric ratio (3:1) of EPON 862 (Diglycidyl Ether of Bisphenol F) resin and TETA (Triethylenetetramine) curing agent, respectively, as shown in Fig. 1.

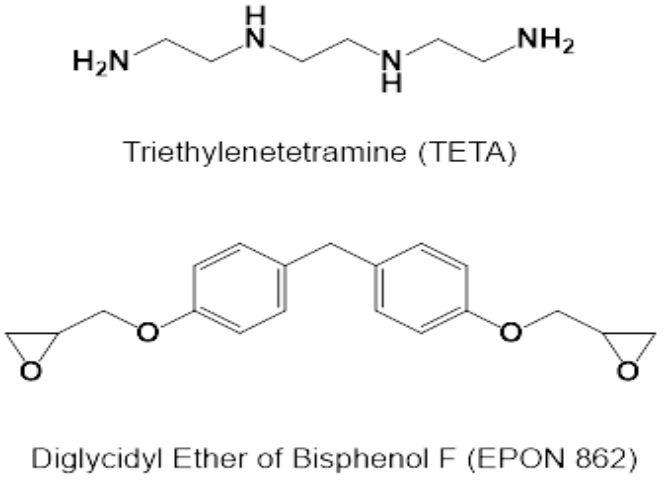

Fig. 1 The atomic structure of the epoxy resin and hardener.

The simulation box of the pure polymer and nanocomposites was constructed using the PACKMOL software[14] so that 130 TETA and 390 EPON molecules were introduced for each one. The nanocomposites RVE was modeled by inserting a (short) zigzag (11,0) CNT with non-periodic boundary conditions at the central position of a rectangular orthogonal box, and the resin and hardener are packed around the CNT as shown in Fig. 2.

The diameter and length of the embedded CNT were 0.861 nm and 9.845 nm, respectively.[15,16] Subsequently, a static cross-linking procedure[17] was used to cure the resin up to 80% using the large-scale atomic/molecular massively parallel simulator (LAMMPS)[18] and an in-house developed code.[15,16,19]

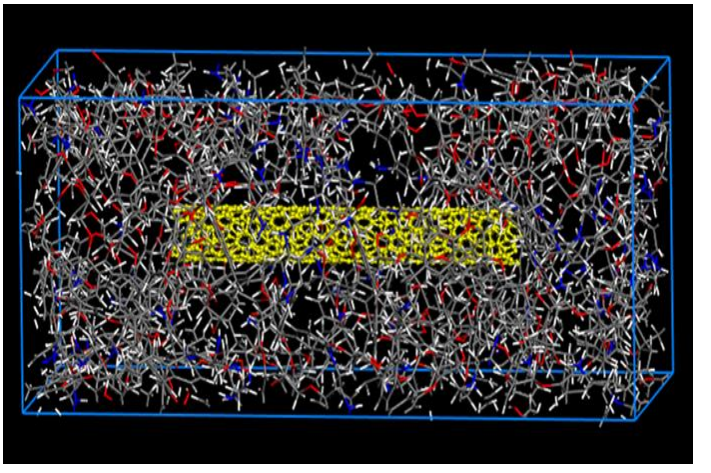

Fig. 2 The initial structure of nanocomposites RVE containing the polymer constituents and CNT.

The cross-linking procedure is based on the static cross-linking process.[17,20-22] The essential assumptions of the curing process involved:

a) The reactivity of primary and secondary amines is the same,

b) The reaction cut-off was selected based on the highest pick in the radial distribution function between the reactive carbon and nitrogen atoms (C-N),

c) After each equilibrium step (50 *ps*), the RVE was checked for a new bond,

d) The constants of new bonds were increased in multiple steps gradually and reached the real values in the bond function of the PCFF force field,[17]

e) The outputs were investigated by an in-house FORTRAN code to introduce topology parameters equivalent to the new bonds,

f) An annealing procedure was applied to relax the RVE structure,

g) The overall procedure (*c*-*f*) was repeated to reach about 80% curing followed by a final equilibration (3 *ns*).

The pure polymer and nanocomposites RVE dimensions were 5.92×5.70×6.15 *nm* and 4.25×4.14×11.54 *nm* after curing and equilibration processes, respectively. All intramolecular and intermolecular interactions in the polymer and nanocomposites RVEs were defined with the polymer consistent force field (PCFF).[23] The PCFF parameters are based on quantum mechanical calculations (Hartree–Fock approximation with the 6-31G* basis set).[23] It has been proven that it can predict nanocomposites RVE.[24,25] The interactions between the CNT and the polymer matrix are very important in load transferring. Therefore, many investigations were performed in which the interfacial interactions were

defined based on the PCFF force field.[24-30] In PCFF, the non-bonded Van der Waals (VdW) interactions with the same atoms (ii) are determined based on the Lennard-Jones (LJ) 9-6 potential with a cutoff radius of 12 Å as follows:

$$V = \varepsilon \left[2\left(\frac{\sigma}{r}\right)^9 - 3\left(\frac{\sigma}{r}\right)^6\right] \qquad r < r_c \qquad (1)$$

where V is the interaction energy, σ is the equilibrium distance,ε is the potential well depth, r is the atomic distance, and r_c is the cut-off radius. The ε and σ between different types (ij) are calculated with a sixth power mixing rule (pair_modify command in LAMMPS) as follows:

$$\varepsilon_{ij} = \frac{2\left(\sqrt{\varepsilon_i \varepsilon_j}\right)\left(\sigma_i^3 \sigma_j^3\right)}{\sigma_i^6 + \sigma_j^6} \quad \sigma_{ij} = \left(\frac{\left(\sigma_i^6 + \sigma_j^6\right)}{2}\right)^{\frac{1}{6}} \qquad (2)$$

The isolated CNT was described based on the adaptive intermolecular reactive empirical bond order (AIREBO). This many-body force field could predict the mechanical behavior of the carbon allotropes properly up to failure which is as follows:

$$E = \frac{1}{2}\sum_i \sum_{i \neq j}\left[E_{ij}^{REBO} + E_{ij}^{LJ} + \sum_{k \neq i,j} \sum_{l \neq i,j,k} E_{kijl}^{TORSION}\right] \qquad (3)$$

where E_{ij}^{REBO} and E_{ij}^{LJ} terms are the REBO potential by Brenner and longer-ranged interactions (2 < r < cutoff) by an equation similar to standard Lennard Jones potential respectively. Also, $E_{kijl}^{TORSION}$ the term defines various explicit 4-body dihedral angles. [31]

The pressure and temperature were controlled using the Nose-Hoover style non-Hamiltonian equations of motion at 1 *atm* and 300 *K*, respectively. The pair cut-off was 1.2 *nm* which is proportional to 2.5σ in the VdW equation of the PCFF force field.[32] The time-step of the simulation was 1 *fs*. An optimized time step will be obtained when it is chosen according to a period of the highest vibrational frequency of the chemical covalent bonds.[33] Also, the results of several simulations show that choosing a 1 *fs* time-step is appropriate and has led to results consistent with experimental findings.[34,35] The value of the strain rate was 10^{-4} ps^{-1}. Many researchers reported that a strain rate equal to 10^{-4} ps^{-1} leads to reliable results.[36-38] The stress components were calculated using the so-called Virial equation. The pull-out test was performed on the equilibrated nanocomposites RVE, in which a portion of polymer in front of the pulling path was removed and the polymer with 0.5 nm thickness at the backside of the embedded CNT was restricted in the pull-out direction Fig. 3. The embedded CNT was pulled out along its axial direction at a constant velocity of 0.0001 Å/fs.[39]

3. Results and discussion

3.1 Validation of the MD model and mechanical behavior of the RVE constituents

The MD model is validated through the analysis of the mechanical behavior of three cases including the isolated CNT and pure polymer block under tensile loads as well as the mechanical response of the CNT/cured epoxy interface through the CNT pullout test, to analyze the interface properties. The stress-strain behaviors of the isolated CNT and pure polymer under tensile load were computed and shown in Figs. 4a-b. The elastic modulus is obtained using the slope of the stress-strain curve. Due to some fluctuation in the curve,

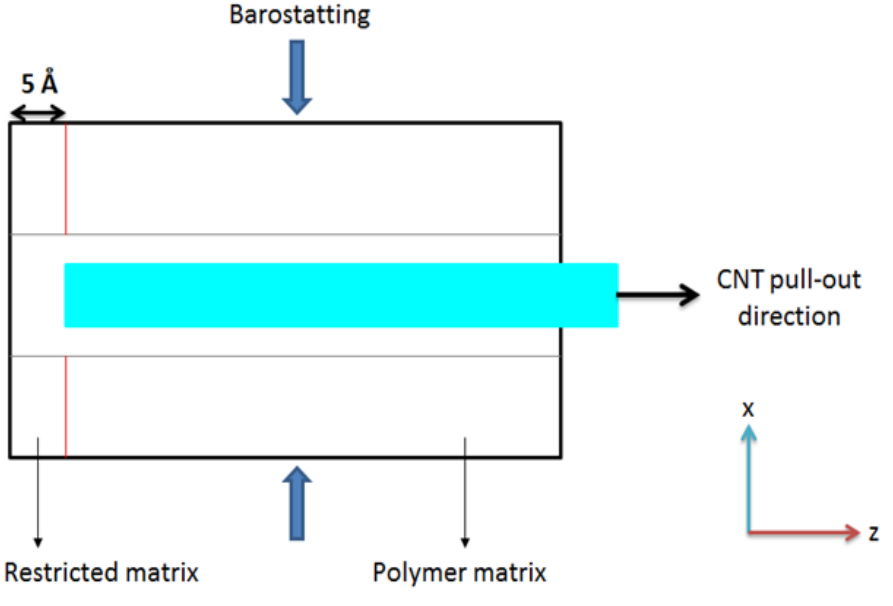

Fig. 3 The schematic view of the RVE condition during the pullout test.

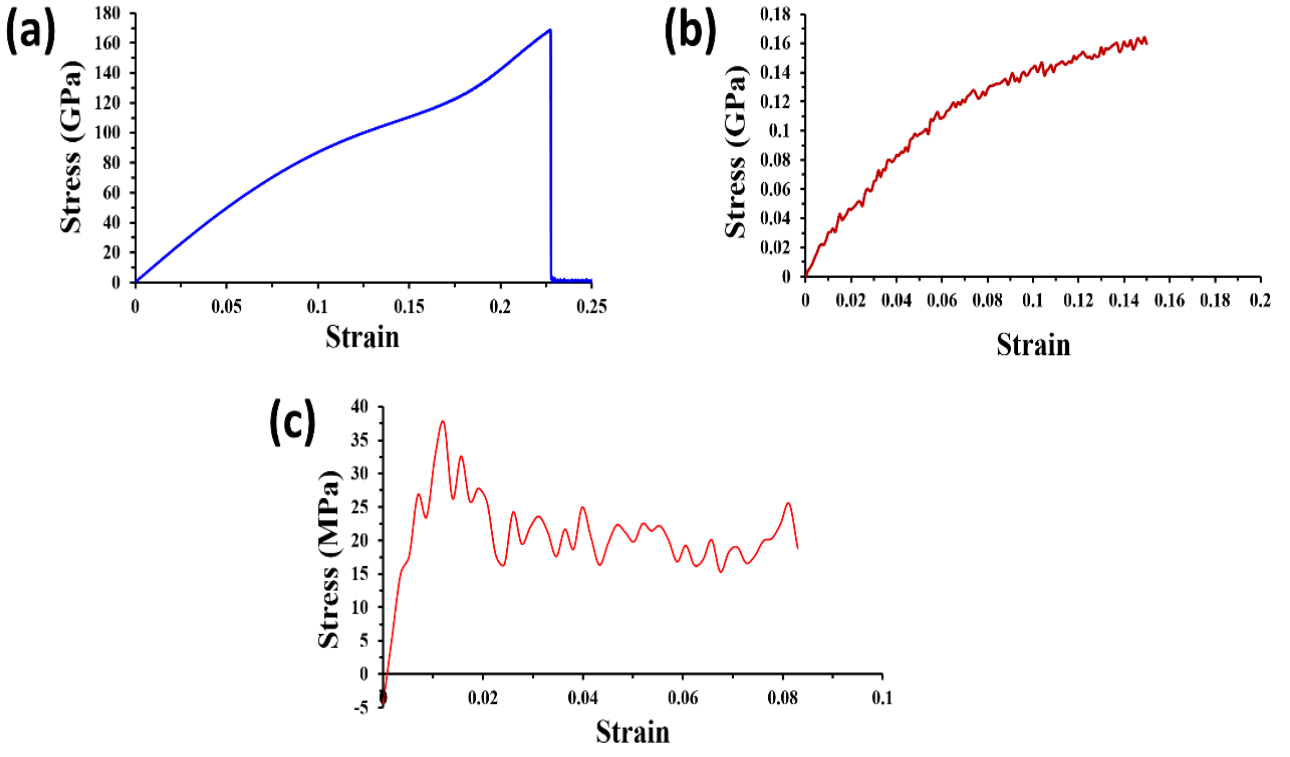

Fig. 4 (a) The stress-strain curves of the isolated CNT under tension, (b) pure polymer under tensile load, and (c) CNT/epoxy interface from the CNT pull-out test.

this modulus is calculated using the least-square approximation.

The mechanical properties of the epoxy polymer are listed in Table 1 and compared with the results of the published experimental counterparts. As can be seen, the results are in good agreement with the other published research works.[15,16,19]

Table 1. Comparison of the polymer properties obtained from this study with reference results.

Property	This study	Other Simulations [40-42]	Experiments [43-44]
Density (g/cm^3)	1.14	1.08-1.16	1.16
Young's modulus (GPa)	2.29-3.24	2.7-3.8	2.4-3.4
Poisson's ratio	0.39	0.28-0.33	0.3-0.4
Shear modulus (GPa)	0.93-1.12	1.04-1.48	1.0-1.5

Through the analysis of the structure, the response of the embedded CNT pull-out from the polymer in a form of the stress-strain curve is obtained as shown in Fig. 4c. In this regard, the initial stress of 37.66 MPa is computed where the slippage phenomenon has occurred in the interface between the embedded CNT and the matrix. The very low value of the interface shear strength denoted a sensitive physical condition of the interface area between the soft polymer matrix and hard-embedded CNT in the form of a stress concentration zone.

The area under the stress-strain curve is the strain energy density that highlights the capacity of materials in energy absorption. The maximum strain energy density of the isolated CNT and polymer are calculated using the area underneath the curves of Fig. 4 as 20223.81 MJ/m^3 and 29.80 MJ/m^3, respectively. On the other hand, the results of the pull-out test show that the dissipation of small strain energy of 17.69 MJ/m^3 could cause interface bond separation that initiates the slippage of the polymer chains on the embedded CNT surface. Results indicated the massive capacity of the CNT to absorb energy in comparison with the strain energies of polymer and CNT/polymer interface which are only 0.15% and 0.09% of that of the isolated CNT.

3.2 Mechanical behavior of CNT/Epoxy nanocomposites and crosslinking effects

The CNT/epoxy nanocomposites consist of four phases; the polymer matrix, CNT/polymer interphase, CNT/polymer interface, and the embedded CNT as illustrated in Fig. 5. As shown in this figure, there are no molecules in the interface, but it is created by VdW forces between the nanotube and polymer. Also, there is an interphase region in which the polymer chain has different arrangements and properties compared to the bulk polymer due to the interaction with the

CNT.

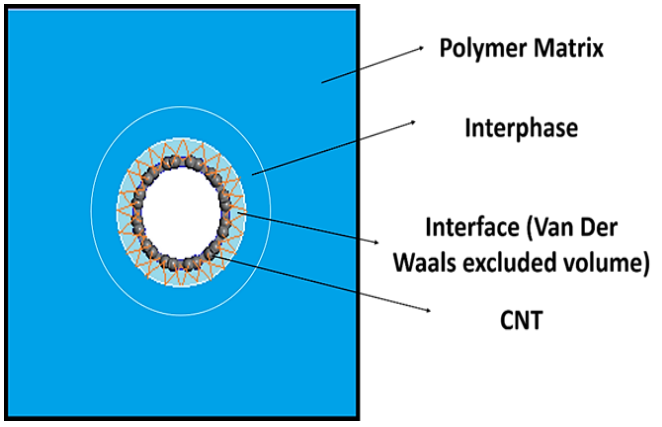

Fig. 5 Schematic illustration of the RVE components that are created due to the VdW interaction between the polymer and the CNT.

The mechanical response of the RVE system, during the curing process, is an interactive response to deformations of these phases. The response of the nanocomposites RVE after the curing process under tensile load, in terms of stress-strain behavior, and the variation of the average longitudinal stress on the embedded CNT are computed as illustrated in Fig. 6a (regions 1 and 2). The slope of the stress-strain curve of the nanocomposites RVE was calculated as the elastic modulus of the RVE, which is obtained from the least-square approximation due to some fluctuation in the curve. The modulus of the nanocomposites is obtained as 3.75 GPa at 2% strain, indicating a 60% improvement in comparison with the modulus of the pure polymer.

In the first phase of the result (region 1, Fig. 6a), initially, a negative value of the longitudinal stress (residual stress = -197 Mpa) was observed on the embedded CNT. When the cross-linking process was finished and the temperature decreased to ambient temperature the residual stresses appeared in the constituents which are induced to the embedded CNT during the polymer cross-linking process in the RVE. The residual stress is computed as up to -33% of the maximum tensile stress experienced by the CNT after loading the RVE. This phenomenon indicates a considerable amount of residual stress in the embedded CNT that must be considered in the simulation process to account for accurate measurement of the RVE properties.

The applied tensile load on both ends of the nanocomposite RVE system caused deformation in the polymer that is transferred to the embedded CNT through the interphase and interface zones. In the process of RVE unit-cell deformation, the load is transferred from the polymer to the embedded CNT through Van der Waals interactions. Through this process, the variation of the interaction force between the CNT and polymer matrix in the interface, as well as stress variation in the polymer phase are shown in Figs. 6b-c.

In Fig. 6a, it can be seen that the interaction force increases to a maximum value and remain constant through the load, and simultaneously the average stress on the embedded CNT increases and reaches a constant value equal to 295 MPa.

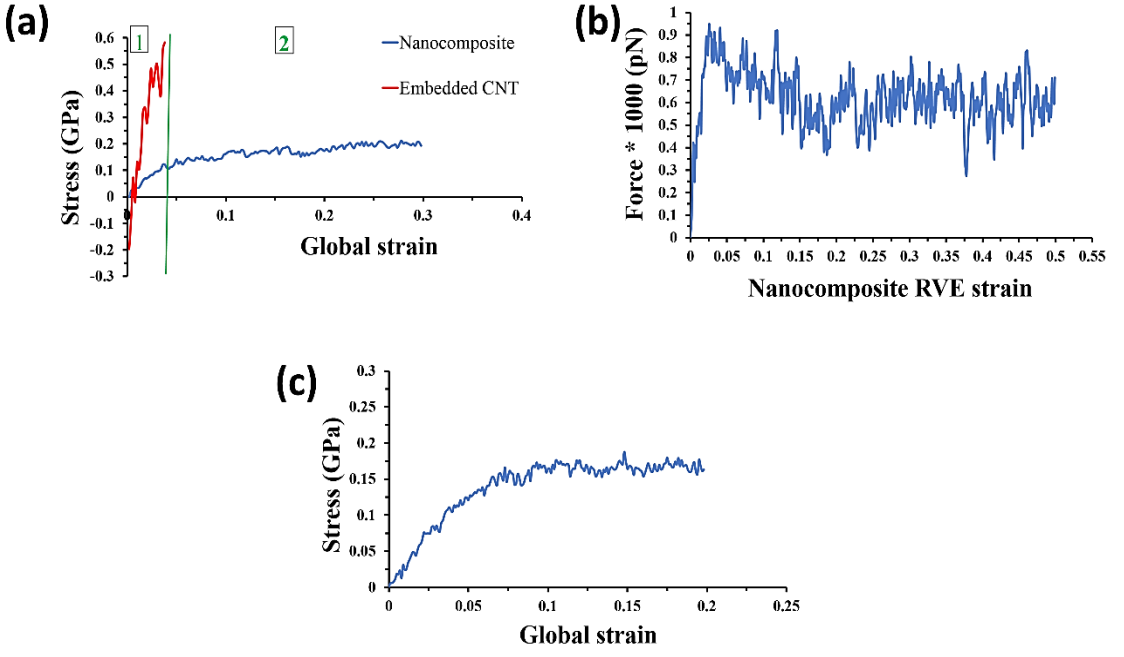

Fig. 6 (a) The stress-strain behavior of the nanocomposite RVE and the variations of average longitudinal stress on the embedded CNT against global strain, (b) the variation of normal load between the embedded CNT and polymer versus the RVE strain, and (c) normal stress on the polymer phase against global strain.

Hence, the internal analysis showed that the deformation in the embedded CNT remains constant with some fluctuation in the stress value in comparison with the polymer displacement which, is due to the discrete nature of atomistic levels. Also, the variation of normal stress rate on the polymer phase reduces to a constant value with a larger strain indicating excessive deformation in the polymer part (Fig. 6c). The slippage between the embedded CNT and polymer chains is another phenomenon that is the result of the shear debonding in the CNT/epoxy interface zone which encounters the creation of new attractive interactions between the CNT and polymer. This phenomenon caused the deformation of the embedded CNT to remain constant within the elastic region at the state where it was expanded and subsequently, the embedded CNT experiences a constant level of longitudinal stress with periodic stress variation, resulting from the Van der Waals attractive and repulsive interaction between the atoms in the interface zone.

4. Conclusions

This study focuses on the mechanical response of CNT/Epoxy nanocomposite RVE that is cured up to 80% bond formation using an in-house code and LAMMPS software. The responses of the isolated CNT, pure polymer under tensile load, and CNT/polymer pull-out test are presented and used for validation of the model and a better understanding of the RVE system response. It was observed that:

- During in situ cross-linking, the embedded CNT shrinks in the longitudinal direction leading to significant residual stress on CNT.
- The analysis of the RVE structure identifies two different states for the mechanical behavior of nanocomposites, including an elastic-linear behavior and a nonlinear response.
- When the polymer behaves within the elastic limit, an equivalent high response was observed by the RVE system resulting from intermolecular and intramolecular interactions of the entire RVE. This result could be considered as the pure elastic response of the nanocomposites RVE system to calculate the elastic modulus and other mechanical properties. In this state, excessive residual stress on CNT is computed after curing as -33% of the maximum stress experienced by CNT. Also, while the RVE system is under 2.5% strain (Fig. 6a), the maximum value of stress in the embedded CNT is predicted 582 MPa which is only 0.05% of the isolated CNT strength (Fig. 4a). Then the polymer undergoes a nonlinear deformation created by the interface slippage phenomenon.
- The mechanical behavior of the RVE system is the reflection of excessive deformation in the polymer constituent as well as the slippage phenomenon in the interface, which establishes the global response of RVE as a unit structure.

Future research: Since many different types of nano-structured reinforcement such as graphene are being used to enhance the properties of polymeric material, a similar process as provided in this study, is recommended for investigation on the effect of curing-induced residual stresses on the mechanical behavior of other types nanocomposites reinforced by other types of nanoparticles.

Acknowledgment

This work was supported by the Iran National Science Foundation, Grant No. 98010610.

Conflict of Interest

There is no conflict of interest.

Supporting Information

Not applicable.

References

[1] M. S. Dresselhaus, G. Dresselhaus, A. Jorio, Unusual properties and structure of carbon nanotubes, *Annual Review of Materials Research*, 2004, **34**, 247–278, doi: 10.1146/annurev.matsci.34.040203.114607.

[2] A. Kausar, I. Rafique, B. Muhammad, Review of applications of polymer/carbon nanotubes and epoxy/CNT composites, *Polymer-Plastics Technology and Engineering*, 2016, **55**, 1167–1191, 10.1080/03602559.2016.1163588.

[3] Jun, Huang, The effect of carbon nanotube orientation and content on the mechanical properties of polypropylene based composites, *Materials & Design*, 2014, **55**, 653-663, doi: 10.1016/j.matdes.2013.10.039.

[4] Z. Hu, M. R. H. Arefin, X. Yan, Q. H. Fan, Mechanical property characterization of carbon nanotube modified polymeric nanocomposites by computer modeling, *Composites Part B: Engineering*, 2014, **56**, 100-108, doi: 10.1016/j.compositesb.2013.08.052.

[5] B. Arash, Q. Wang, V. K. Varadan, Mechanical properties of carbon nanotube/polymer composites, *Scientific Reports*, 2014, **4**, 6479, doi: 10.1038/srep06479.

[6] P. Padhi, K. N. Kumar, S. Ghosh, H. Vishwanatha, S. C. Panigrahi, S. Ghosh, Modeling and experimental validation of deagglomeration of ultrafine nanoparticles in liquid Al during noncontact ultrasonic casting of Al–Al_2O_3 nanocomposite, *Materials and Manufacturing Processes*, 2016, **31**, 1589 - 1596, doi: 10.1080/10426914.2015.1004707.

[7] N. K. Kottana, H. M. Vishwanatha, S. Sengupta, K. Saxena,

A. Behera, S. Ghosh, Investigation on synergetic effect of non-contact ultrasonic casting and mushy state rolling on microstructure and hardness of Al-Si-Al_2O_3 nanocomposites, *International Journal on Interactive Design and Manufacturing (IJIDeM)*, 2022, 1-10, doi: 10.1007/s12008-022-00986-y.

[8] X. Chen, A. R. Alian, S. A. Meguid, Modeling of CNT-reinforced nanocomposite with complex morphologies using modified embedded finite element technique, *Composite Structures*, 2019, **227**, 111329, doi: 10.1016/j.compstruct.2019.111329.

[9] X. Lu, A. Zhang, O. Dubrunfaut, D. He, L. Pichon, J. Bai, Numerical modeling and experimental characterization of the AC conductivity and dielectric properties of CNT/polymer nanocomposites, *Composites Science and Technology*, 2020, **194**, 108150, doi: 10.1016/j.compscitech.2020.108150.

[10] M. K. Hassanzadeh-Aghdam, M. J. Mahmoodi, R. Ansari, H. Mehdipour, Effects of adding CNTs on the thermo-mechanical characteristics of hybrid titanium nanocomposites, *Mechanics of Materials*, 2019, **131**, 121-135, doi: 10.1016/j.mechmat.2019.01.022.

[11] Y. Li, G. Seidel, Multiscale modeling of functionalized interface effects on the effective elastic material properties of CNT–polyethylene nanocomposites, *Computational Materials Science*, 2015, **107**, 216-234, doi: 10.1016/j.commatsci.2015.05.006.

[12] X. Peng, S.A. Meguid, Molecular dynamics simulations of the buckling behavior of defective carbon nanotubes embedded in epoxy nanocomposites, *European Polymer Journal*, 2017, **93**, 246–258, 10.1016/j.eurpolymj.2017.06.010.

[13] C. Li, A. R. Browning, S. Christensen, A. Strachan, Atomistic simulations on multilayer graphene reinforced epoxy composites, *Composites Part A: Applied Science and Manufacturing*, 2012, **43**, 1293-1300, doi: 10.1016/j.compositesa.2012.02.015.

[14] L. Martínez, R. Andrade, E. G. Birgin, J. M. Martínez, PACKMOL: A package for building initial configurations for molecular dynamics simulations, *Journal of Computational Chemistry*, 2009, **30**, 2157-2164, doi: 10.1002/jcc.21224.

[15] S.M. Rahimian-Koloor, S. M. Hashemianzadeh, M.M. Shokrieh, Effect of CNT structural defects on the mechanical properties of CNT/Epoxy nanocomposite, *Physica B: Condensed Matter*, 2018, **540**, 16-25, doi: 10.1016/j.physb.2018.04.012.

[16] S. M. Rahimian-Koloor, H. Moshrefzadeh-Sani, M. M. Shokrieh, S. M. Hashemianzadeh, On the behavior of isolated and embedded carbon nano-tubes in a polymeric matrix, *Materials Research Express*, 2018, **5**, 25019, 10.1088/2053-1591/aaac4e.

[17] V. Varshney, S. S. Patnaik, A. K. Roy, B. L. Farmer, A molecular dynamics study of epoxy-based networks: cross-linking procedure and prediction of molecular and material properties, *Macromolecules*, 2008, **41**, 6837-6842, doi: 10.1021/ma801153e.

[18] S. Plimpton, Fast parallel algorithms for short-range molecular dynamics, *Journal of Computational Physics*, 1995, **117**, 1-19, doi: 10.1006/jcph.1995.1039.

[19] S. M. Rahimian-Koloor, H. Moshrefzadeh-Sani, S. M. Hashemianzadeh, M. M. Shokrieh, The effective stiffness of an embedded graphene in a polymeric matrix, *Current Applied Physics*, 2018, **18**, 559-566, doi: 10.1016/j.cap.2018.02.007.

[20] C. M. Hadden, B. D. Jensen, A. Bandyopadhyay, G. M. Odegard, A. Koo, R. Liang, Molecular modeling of EPON-862/graphite composites: Interfacial characteristics for multiple crosslink densities, *Composites Science and Technology*, 2013, **76**, 92-99, doi: 10.1016/j.compscitech.2013.01.002.

[21] I. Yarovsky, Computer simulation of structure and properties of crosslinked polymers: application to epoxy resins, *Polymer*, 2002, **43**, 963-969, doi: 10.1016/s0032-3861(01)00634-6.

[22] C. Wu, W. Xu, Atomistic molecular modelling of crosslinked epoxy resin, *Polymer*, 2006, **47**, 6004-6009, doi: 10.1016/j.polymer.2006.06.025.

[23] H. Sun, S. J. Mumby, J. R. Maple, A. T. Hagler, An ab initio CFF93 all-atom force field for polycarbonates, *Journal of the American Chemical Society*, 1994, **116**, 2978-2987, doi: 10.1021/ja00086a030.

[24] F. Liu, N. Hu, M. Han, S. Atobe, H. Ning, Y. Liu, L. Wu, Investigation of interfacial mechanical properties of graphene-polymer nanocomposites, *Molecular Simulation*, 2016, **42**, 1165–1170, 10.1080/08927022.2016.1154550.

[25] V. Lordi, N. Yao, Molecular mechanics of binding in carbon-nanotube-polymer composites, *Journal of Materials Research*, 2000, **15**, 2770-2779, doi: 10.1557/JMR.2000.0396.

[26] R. Rahman, A. Haque, Molecular dynamics simulation of cross-linked graphene-epoxy nanocomposites, *arXiv preprint arXiv:1108.2826*, 2011.

[27] F. Liu, N. Hu, H. Ning, Y. Liu, Y. Li, L. Wu, Molecular dynamics simulation on interfacial mechanical properties of polymer nanocomposites with wrinkled graphene, *Computational Materials Science*, 2015, **108**, 160-167, doi: 10.1016/j.commatsci.2015.06.023.

[28] R, Rahman, Molecular modeling of crosslinked graphene-epoxy nanocomposites for characterization of elastic constants and interfacial properties, *Composites Part B: Engineering*, 2013, **54**, 353-364, doi: 10.1016/j.compositesb.2013.05.034.

[29] R. Rahman, The role of graphene in enhancing the stiffness of polymeric material: a molecular modeling approach, *Journal of Applied Physics*, 2013, **113**, 243503, doi: 10.1063/1.4812275.

[30] Z. Yuan, Z. Lu, Z. Yang, J. Sun, F. Xie, A criterion for the normal properties of graphene/polymer interface, *Computational Materials Science*, 2016, **120**, 13–20, doi:10.1016/j.commatsci.2016.04.006.

[31] S. Stuart, A. B. Tutein, J. Harrison, A reactive potential for hydrocarbons with intermolecular interactions, *Journal of Chemical Physics*, 2000, **112**, 6472-6486, doi: 10.1063/1.481208.

[32] D. Frenkel, B. Smit, M. A. Ratner, Understanding molecular simulation: from algorithms to applications, *Physics Today*, 1997, **50**, 66, doi: 10.1063/1.881812.

[33] A. R. Leach, Molecular Modelling: Principles and Applications. Pearson, Second Edition, 2001.

[34] S. S. R. Koloor, S. M. Rahimian-Koloor, A. Karimzadeh, M. Hamdi, M. Petrů, M. N. Tamin, Nano-level damage characterization of graphene/polymer cohesive interface under

tensile separation, *Polymers*, 2019, **11**, 1435, doi: 10.3390/polym11091435.
[35] J. Choe, B. Kim, Determination of proper time step for molecular dynamics simulation, *Bulletin of the Korean Chemical Society*, 2000, **21**, 419-424.
[36] N. Shenogina, M. Tsige, S. Patnaik, S. Mukhopadhyay, Molecular modeling of elastic properties of thermosetting polymers using a dynamic deformation approach, *Polymer*, 2013, **54**, 3370-3376, doi: 10.1016/J.POLYMER.2013.04.034.
[37] D. Hossain, M. Tschopp, D. Ward, J. Bouvard, P. T. Wang, M. Horstemeyer, Molecular dynamics simulations of deformation mechanisms of amorphous polyethylene, *Polymer*, 2010, **51**, 6071-6083, 10.1016/j.polymer.2010.10.009.
[38] S. Yang, S. Yu, M. Cho, Influence of Thrower–Stone–Wales defects on the interfacial properties of carbon nanotube/polypropylene composites by a molecular dynamics approach, *Carbon N. Y.*, 2013, **55**, 133-143, 10.1016/j.carbon.2012.12.019.
[39] A. R. Alian, S. A. Meguid, Molecular dynamics simulations of the effect of waviness and agglomeration of CNTs on interface strength of thermoset nanocomposites, *Physical Chemistry Chemical Physics*, 2017, **19**, 4426-4434, doi: 10.1039/c6cp07464b.
[40] F. Aghadavoudi, H. Golestanian, Y. Tadi Beni, Investigating the effects of resin crosslinking ratio on mechanical properties of epoxy-based nanocomposites using molecular dynamics, *Polymer Composites*, 2016, **38**, E433-E442, doi: 10.1002/pc.24014.
[41] C. Li, A. Strachan, Molecular simulations of crosslinking process of thermosetting polymers, *Polymer*, 2010, **51**, 6058-6070, doi: 10.1016/j.polymer.2010.10.033.
[42] A. Shokuhfar, B. Arab, The effect of cross linking density on the mechanical properties and structure of the epoxy polymers: molecular dynamics simulation, *Journal of Molecular Modeling*, 2013, **19**, 3719-3731, doi: 10.1007/s00894-013-1906-9.
[43] E. N. Brown, S. R. White, N. R. Sottos, Microcapsule induced toughening in a self-healing polymer composite, *Journal of Materials Science*, 2004, **39**, 1703-1710, doi: 10.1023/B:JMSC.0000016173.73733.dc.
[44] F. Garcia, B. G. Soares, V. Pita, R. Sánchez, J. Rieumont, Mechanical properties of epoxy networks based on DGEBA and aliphatic amines, *Journal of Applied Polymer Science*, 2007, **106**, 2047-2055, doi: 10.1002/APP.24895.

